



Oligomer β -amyloid Induces Hyperactivation of Ras to Impede NMDA Receptor-Dependent Long-Term Potentiation in Hippocampal CA1 of Mice

Ya Wang¹, Zhaochun Shi², Yajie Zhang¹, Jun Yan³, Wenfeng Yu^{4*} and Ling Chen^{1*}

¹Department of Physiology, Nanjing Medical University, Nanjing, China, ²Department of Neurology, First Affiliated Hospital of Nanjing Medical University, Nanjing, China, ³Department of Geriatric Medicine, Affiliated Nanjing Brain Hospital of Nanjing Medical University, Nanjing, China, ⁴Key Laboratory of Endemic and Ethnic Diseases of Education Ministry, Guizhou Medical University, Guizhou, China

OPEN ACCESS

Edited by:

Filippo Caraci,
University of Catania, Italy

Reviewed by:

Igor Klyubin,
Trinity College Dublin, Ireland
Antonio De Iure,
San Raffaele Pisana (IRCCS), Italy

*Correspondence:

Ling Chen
lingchen@njmu.edu.cn
Wenfeng Yu
wenfengyu2013@126.com

Specialty section:

This article was submitted to
Experimental Pharmacology and
Drug Discovery,
a section of the journal
Frontiers in Pharmacology

Received: 28 August 2020

Accepted: 20 October 2020

Published: 10 December 2020

Citation:

Wang Y, Shi Z, Zhang Y, Yan J, Yu W
and Chen L (2020) Oligomer β -amyloid
Induces Hyperactivation of Ras to
Impede NMDA Receptor-Dependent
Long-Term Potentiation in
Hippocampal CA1 of Mice.
Front. Pharmacol. 11:595360.
doi: 10.3389/fphar.2020.595360

The activity of Ras, a small GTPase protein, is increased in brains with Alzheimer's disease. The objective of this study was to determine the influence of oligomeric $A\beta_{1-42}$ on the activation of Ras, and the involvement of the Ras hyperactivity in $A\beta_{1-42}$ -induced deficits in spatial cognition and hippocampal synaptic plasticity. Herein, we show that intracerebroventricular injection of $A\beta_{1-42}$ in mice ($A\beta$ -mice) enhanced hippocampal Ras activation and expression, while 60 min incubation of hippocampal slices in $A\beta_{1-42}$ ($A\beta$ -slices) only elevated Ras activity. $A\beta$ -mice showed deficits in spatial cognition and NMDA receptor (NMDAR)-dependent long-term potentiation (LTP) in hippocampal CA1, but basal synaptic transmission was enhanced. The above effects of $A\beta_{1-42}$ were corrected by the Ras inhibitor farnesylthiosalicylic acid (FTS). ERK2 phosphorylation increased, and Src phosphorylation decreased in $A\beta$ -mice and $A\beta_{1-42}$ -slices. Both were corrected by FTS. In CA1 pyramidal cells of $A\beta_{1-42}$ -slices, the response of AMPA receptor and phosphorylation of GluR1 were enhanced with dependence on Ras activation rather than ERK signaling. In contrast, NMDA receptor (NMDAR) function and GluN2A/2B phosphorylation were downregulated in $A\beta_{1-42}$ -slices, which was recovered by application of FTS or the Src activator ouabain, and mimicked in control slices treated with the Src inhibitor PP2. The administration of PP2 impaired the spatial cognition and LTP induction in control mice and FTS-treated $A\beta$ -mice. The treatment of $A\beta$ -mice with ouabain rescued $A\beta$ -impaired spatial cognition and LTP. Overall, the results indicate that the oligomeric $A\beta_{1-42}$ hyperactivates Ras and thereby causes the downregulation of Src which impedes NMDAR-dependent LTP induction resulting in cognitive deficits.

Keywords: Alzheimer's disease, amyloid beta, spatial cognition, NMDA receptor, farnesylthiosalicylic acid, Ras-GTP

HIGHLIGHTS

- (1) Ras activity is increased by *in vivo* or *in vitro* A β_{1-42} application.
- (2) Ras inhibitor FTS relieves A β -impaired cognition and NMDAR-dependent LTP.
- (3) Ras hyperactivation *via* suppressed Src activity impedes NMDAR function.
- (4) Src inhibitor can impair cognition and LTP in control mice and FTS/A β_{1-42} mice.
- (5) Src activator rescues A β -impaired spatial cognition and NMDAR-dependent LTP.

1. INTRODUCTION

AD is the most frequent cause of dementia in the elderly, featured by progressive loss of memory and amyloid β (A β) peptides accumulation in the brain. The injection of synthetic A β_{1-42} into the brain or overexpression of A β -generating fragments causes learning and memory deficits in various models, indicating a connection between A β accumulation and dementia. However, it remains to be clarified how these actions of oligomeric A β_{1-42} impair learning and memory, since the memory deficits at early stages of A β accumulation are not always associated with massive neuronal degeneration and loss.

High level of Ras, a small GTPase superfamily protein, is found in brains with AD (McShea et al., 2007). Isoprenylated GTPases have been reported to involve in the pathogenesis of AD (Ostrowski et al., 2007; Scheper et al., 2007). Ras interacts with its guanine nucleotide exchange factor to facilitate the conversion of inactive Ras-GDP to active Ras-GTP (Prior and Hancock 2012). Elevated Ras levels were found in early stages of AD (Gartner et al., 1999; Kirouac et al., 2017). The hyperactivation of Ras leads to the disorder of LTP induction (Stornetta and Zhu 2011). The localization of Ras and phosphorylated ERK were increased in plaques and tangles of AD brains (Ferrer et al., 2001; Pei et al., 2002). The Ras-MAPK signaling pathway has been found prior to the formation of plaques and tangles (Gartner et al., 1999) and to influence LTP formation (Ohno et al., 2001). Patients with neurofibromatosis type I (NF1) caused by loss-of-function mutations in the NF1 oncogene have hyperactive Ras, and most NF1 children have cognitive deficits (North et al., 2002). The pharmacological suppression of Ras signaling reverses the deficits in learning in mouse models of NF1 (Li et al., 2005; Cui et al., 2008). However, whether or how hyperactivation of Ras is involved in A β_{1-42} -induced cognitive deficits remains to be elucidated.

An earlier study reported that tyrosine phosphorylation of NMDA receptors (NMDARs) was enhanced in mice lacking H-Ras (Manabe et al., 2000). Src is a novel H-Ras binding partner. The activation of Ras has been found to modify the downstream effector Src (Thornton et al., 2003). Hippocampal Src kinase activity was increased by H-Ras deficiency, and

subsequently enhanced NMDAR function and facilitated LTP induction (Thornton et al., 2003). The administration of farnesyl transferase inhibitor in mice can enhance NMDAR GluN2A/GluN2B phosphorylation through enhanced Src signaling (Chen et al., 2016). Farnesylthiosalicylic acid (FTS), a synthetic Ras inhibitor (Kloog et al., 1999), can dislodge Ras from its anchorage domains to prevent Ras-membrane interactions (Niv et al., 2002). The administration of FTS in mice through enhancing Src activity increases GluN2A/2B phosphorylation (Wang et al., 2018). The inhibition of Ras activity restored normal spine structural plasticity and presynaptic glutamate release in A β -treated neurons (Ye and Carew 2010). Therefore, it is speculated that oligomeric A β_{1-42} impedes NMDAR-dependent LTP induction via Ras hyperactivity, resulting in cognitive deficits.

The objective of this study was to determine whether oligomeric A β_{1-42} affects the activation of hippocampal Ras, and then to investigate how the hyperactivity of Ras is involved in A β_{1-42} -induced damages in spatial cognition and hippocampal CA1 LTP induction, and to explore the underlying molecular mechanisms. Our results indicate that the oligomeric A β_{1-42} causes hyperactivation of Ras, which in turn leads to the downregulation of Src to impede hippocampal NMDAR-dependent LTP induction, resulting in cognitive deficits.

2. MATERIALS AND METHODS

2.1. Experimental Animals

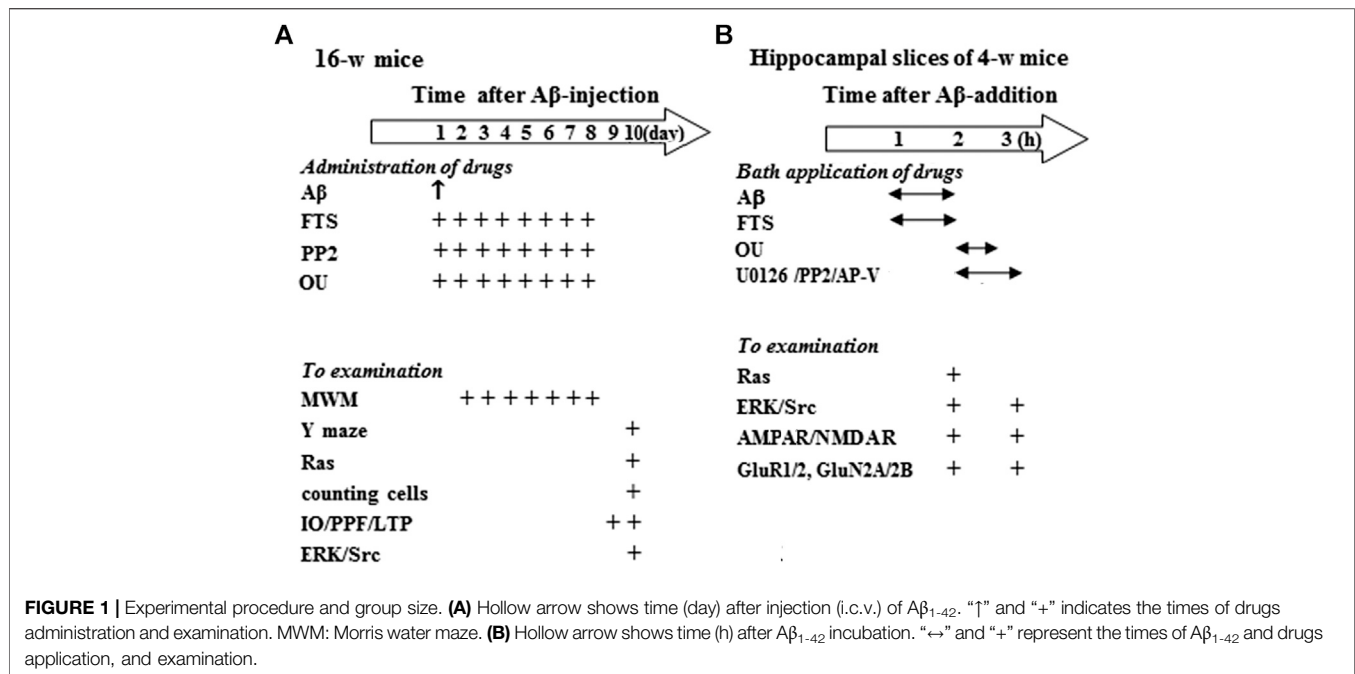
All animal experiments complied with the ARRIVE guidelines, and were performed according to the National Institutes of Health guide for the care and use of Laboratory animals (NIH Publications No. 8023, revised 1978). 16-week-old (39.8 \pm 1.2 g) and 4-week-old (17.8 \pm 1.1 g) male mice (ICR) were in a regulated environment with a 12 h light/dark cycle (lights on at 9:00 A.M.).

2.2. Drug Administration

A β_{1-42} and 1, 1, 1, 3, 3, 3-hexa-fluoro-2-propanol (HFIP) were purchased from Sigma (St. Louis, United States). The A β_{1-42} was dissolved in HFIP and then flash-frozen in liquid nitrogen and lyophilized (Bouter et al., 2013). Lyophilized A β_{1-42} was again dissolved in NaOH (100 mM) (Jin et al., 2016). The 16-week-old mice were given the intracerebroventricular (i.c.v.) injection of oligomeric A β_{1-42} at the dose of 0.1 nmol/2 μ l/side, a non-neurotoxic concentration (Qian et al., 2016). After A β_{1-42} injection, the needle was left for over 5 min.

FTS (Cayman chemical, Ann Arbor, USA) was injected (i.p.) at a dose of 3 mg/kg, because this dose of FTS was effective and could enter the brain within 20 to 30 min (Shohami et al., 2003). In *in vitro* experiments, FTS (4.5 μ M) could inhibit Ras activity (Kloog et al., 1999), thus this study used five μ M FTS to treat hippocampal slices.

NMDAR antagonist AP-5, MEK inhibitor U0126, Src-family kinases (SFKs) inhibitor PP2 and the Src activator ouabain (OU) were purchased from Sigma (St. Louis, USA). The slices were treated with PP2 (20 μ M) (Karni et al., 2003), AP-5 (20 μ M), U0126 (10 μ M) and ouabain (5 μ M) (Tian et al., 2006). PP2 is



reported to pass through the blood-brain barrier in some special animal models (Schumann et al., 2008). However, the injection (i.p.) of PP2 at the dose (0.03 mg/kg) did not alter the levels of NMDAR GluN2A/2B phosphorylation in hippocampus (Sha et al., 2015). In this study, the mice were treated daily with the injection (i.c.v.) of PP2 (1.2 nmol/3 μ l per mouse) for eight consecutive days. For repeated injection (i.c.v.), mice were anesthetized with an injection (i.p.) of ketamine (100 mg/kg)/xylazine (10 mg/kg), and placed into a stereotaxic frame (Stoelting). A small hole (2 mm diameter) was drilled in the skull using a dental drill. A stainless steel guide cannula (26-G, Plastics One, Inc., Roanoke, VA) was implanted in the right lateral ventricle (0.22 mm caudal to bregma, 1 mm lateral to the midline, and 1 mm ventral to the pial surface) and anchored to the skull with stainless steel screws and dental cement. On day three after surgery, PP2 was injected using an infusion cannula (30-G) coupled to a motorized injector (Stoelting, Wood Dale, IL, USA) at a rate of 0.5 μ L/min. The infusion cannula was left in place for 5 min after injection. Control mice were treated with the injection (i.c.v.) of vehicle (same volume). Ouabain, was administered intraperitoneally at the dose of 1 μ g/kg to mice subjected to traumatic brain injury, could improve the neurological function (Dvela-Levitt et al., 2014). In this study, the mice were injected (i.p.) daily with ouabain (1 μ g/kg).

2.3. Experimental Groups and Sample Size

Sixteen-week-old mice including control mice (n = 40), FTS-mice (n = 24), A β_{1-42} -mice (n = 44), A β_{1-42} /FTS-mice (n = 36), PP2-mice (n = 12), A β_{1-42} /FTS/PP2-mice (n = 12), ouabain-mice (n = 12) and A β_{1-42} /ouabain-mice (n = 12) were divided into following groups (Figure 1A). The first group (32 control mice, 20 FTS-mice, 36 A β_{1-42} -mice, 28 A β_{1-42} /FTS-mice, eight PP2-mice, eight A β_{1-42} /FTS/PP2-mice, eight ouabain-mice and eight A β_{1-42} /

ouabain-mice) was used to examine the spatial cognitive behaviors, surviving pyramidal cells, Ras activity and ERK/Src phosphorylation. The second group (8 control mice, 4 FTS-mice, eight A β_{1-42} -mice, eight A β_{1-42} /FTS-mice, four PP2-mice, four A β_{1-42} /FTS/PP2-mice, four ouabain-mice and four A β_{1-42} /ouabain-mice) was used to examine synaptic transmission and LTP induction.

Hippocampal slices (approximately four to five slices per mouse) obtained from 4-week-old control mice (n = 136) were treated with A β_{1-42} and various drugs or vehicle, and then divided into two experimental groups (Figure 1B): The first group was used to examine Ras activities, ERK/Src phosphorylation, expression and phosphorylation of GluR1/2 or GluN2A/2B; the second group was used to examine AMPAR/NMDAR function.

2.4. Behavior Analysis

Morris water maze task (MWM): A pool (diameter = 120 cm) was prepared with black-colored plastic. The water temperature (22 \pm 1 $^{\circ}$ C) of pool was regulated using a bath heater. For the hidden-platform test, a cylindrical dark-colored platform (diameter = 7 cm) was placed in 0.5 cm below the water surface. The trial was stopped when the mouse did not reach the platform within 90 s. Each mouse started pseudorandomly from one of four quadrants. Four trials with an interval of 30 min were conducted each day. The probe trial was performed after the hidden-platform test at 24 h. A computer with a video camera system was used to record the swimming paths and time. In the hidden-platform test, latency to reach the platform and swimming speed were measured.

Y-maze task: The mouse could move freely within 8 min. When the hind paws were completely placed in the arm, arm entry was counted. Alternation was determined as successive

entries into the three arms on overlapping triplet sets. The percentage alternation was calculated as the ratio of actual to possible alternations (defined as the total number of arm entries minus two).

2.5. Histological Examination and Analysis

After anesthetized with ketamine (100 mg/kg)/xylazine (10 mg/kg, i. p.), the mice were perfused transcardially with 4% paraformaldehyde. The removed brains were postfixed overnight in the 4% paraformaldehyde. The paraffin embedding was processed, and then the coronal sections (5 μ m) were cut. The hippocampal sections were stained by toluidine blue. We used a conventional light microscope (Olympus DP70, Japan, \times 40) to observe the hippocampal pyramidal cells. For the analysis of cell quantification, every fourth section was stained by toluidine blue. The healthy pyramidal cells was counted throughout hippocampal CA1 regions ($n = 10$ sections per brain) using the manual tag function of Image Pro-Plus 6 (Media Cybernetics). The density of cells was expressed as cell number per square millimeter (Dawson et al., 2003).

2.6. Electrophysiological Analysis

Slice preparations: Hippocampal slices were obtained from 16-week-old mice for field potential recording or 4-week-old mice for whole cell patch-clamp recording. The brains were kept in ice-cold and oxygenated ACSF (in mM: NaCl 126, CaCl₂ 1, KCl 2.5, MgCl₂ 1, NaHCO₃ 26, KH₂PO₄ 1.25, and D-glucose 20, pH: 7.4) for 10 min. The coronal slices (400 μ m) of hippocampus were cut using a vibrating microtome. The slices were recovered for 1 h, and then transferred to a recording chamber of 30 ± 1 °C.

Field potential recording: For recording hippocampal CA3-CA1 synaptic properties, a bipolar tungsten electrode was placed in CA1 *str. radiatum* to stimulate Schaffer collateral afferents using a stimulator. Excitatory postsynaptic potential (EPSP) was recorded in CA1 *str. radiatum* by a 4–5 M Ω resistance glass microelectrode. 1) Input/output (I/O) curve: EPSP slopes were plotted against various stimulus intensities (0.1–1.1 mA). 2) Paired-pulse facilitation (PPF) was evoked by two stimuli with inter-pulse interval (IPI) of 50–100 ms. The value of paired-pulse ratio (PPR) = EPSP_{S2}/EPSP_{S1} \times 100. The EPSP_{S1} and EPSP_{S2} represented the two stimuli-induced EPSP slopes. 3) High-frequency stimulation (HFS, 100 Hz, 1 s) was delivered to induce LTP.

Cell patch-clamp recording: AMPA-evoked currents (I_{AMPA}) and NMDA-evoked currents (I_{NMDA}) were induced in hippocampal CA1 pyramidal cells using a picospritzer (rapid drug delivery system) and recorded using an EPC-10 amplifier (HEKA Elektronik, Germany) as described (Zhou et al., 2016; Wang et al., 2018). A glass pipette was filled with an internal solution (pH 7.2) (in mM: Cs-gluconate 120, NaCl 2, MgCl₂ 4, Na₂-ATP 4, HEPES 10, EGTA 10). The holding potential was kept at -60 mV. I_{AMPA} was induced by AMPA (1–300 μ M) in the same neuron to produce dose-response curve. To record I_{NMDA} , the slices were perfused with the oxygenated magnesium-free ACSF. NMDA (1–1,000 μ M) was applied to I_{NMDA} . The AMPAR

antagonist CNQX (5 μ M) or the NMDAR antagonist AP-5 (20 μ M) was used to verify the obtained I_{AMPA} and I_{NMDA} .

2.7. Western Blot Analysis

The ketamine (100 mg/kg)/xylazine (10 mg/kg, i. p.) were used to anesthetize mice. After the mice were decapitated, the hippocampus were rapidly removed and homogenized in a lysis buffer (in mM: Tris-HCl 50, NaCl 150, EDTA 5, NaF 10, sodium orthovanadate 1, phenylmethylsulfonyl fluoride 1, 1% Triton X-100, 0.5% sodium deoxycholate and protease inhibitor cocktail). After that, total proteins (20 μ g) were separated by SDS-PAGE and blotted onto a polyvinylidene fluoride (PVDF) membrane. The membranes were incubated in antibodies of phospho-ERK1/2 (1:1,000; CST, USA); phospho-GluR1, phospho-GluR2, phospho-GluN2A and phospho-GluN2B (1:1,000; Abcam, United Kingdom); phospho-Src (1:1,000; Millipore, USA). After visualization, the membranes were treated with stripping buffer (Restore; Pierce) for 15 min, and then incubated with antibodies of ERK1/2 (1:1,000; CST, USA); GluR1, GluR2, GluN2A and GluN2B (1:1,000; Abcam, United Kingdom); Src (1:1,000; Millipore, USA) or β -actin (1:1,000; CST, USA). Ras activation assay was implemented according to the instructions of the company (Cell Biolabs). The small GTPase is tested by Western blot using a target-specific antibody included in the kit.

2.8. Data Analysis

SPSS software was used to perform Statistical analyses. The data were expressed as the means \pm standard error (SE). Repeated measures ANOVA were used to analyze the behavioral and electrophysiological data. The actual values of the ANOVAs (one-way ANOVA, two-way ANOVA, repeated measures ANOVA) followed by Bonferroni post hoc analysis are shown in the section of Results. Differences at $p < 0.05$ were considered statistically significant.

3. RESULTS

3.1. A β_{1-42} Impairs Spatial Cognition Through Enhanced Ras Activation

Spatial cognitive behaviors were examined in mice injected (i.c.v.) with A β_{1-42} (A β -mice) ($n = 8$ per group; **Figure 1A**). The repeated measures ANOVA revealed a progressive decline in the escape latency to reach the hidden platform in the MWM with training days in all groups ($F_{(4, 112)} = 41.460$, $p < 0.001$; **Figure 2A**). In comparison with control mice, the escape latency was significantly increased in A β -mice ($F_{(1, 14)} = 13.095$, $p = 0.003$) without changes in swimming speed ($p > 0.05$). A probe trial was carried out to measure the swimming time spent in four quadrants. Notably, the swimming time in the target quadrant was reduced in A β -mice compared with control mice ($p = 0.042$; **Figure 2B**). In Y-maze, the alternation ratio in A β -mice was lower compared with control mice ($p = 0.038$; **Figure 2C**).

The Ras-GTP pull-down assay using a Ras effector protein that recognizes the active state of Ras was performed to examine the

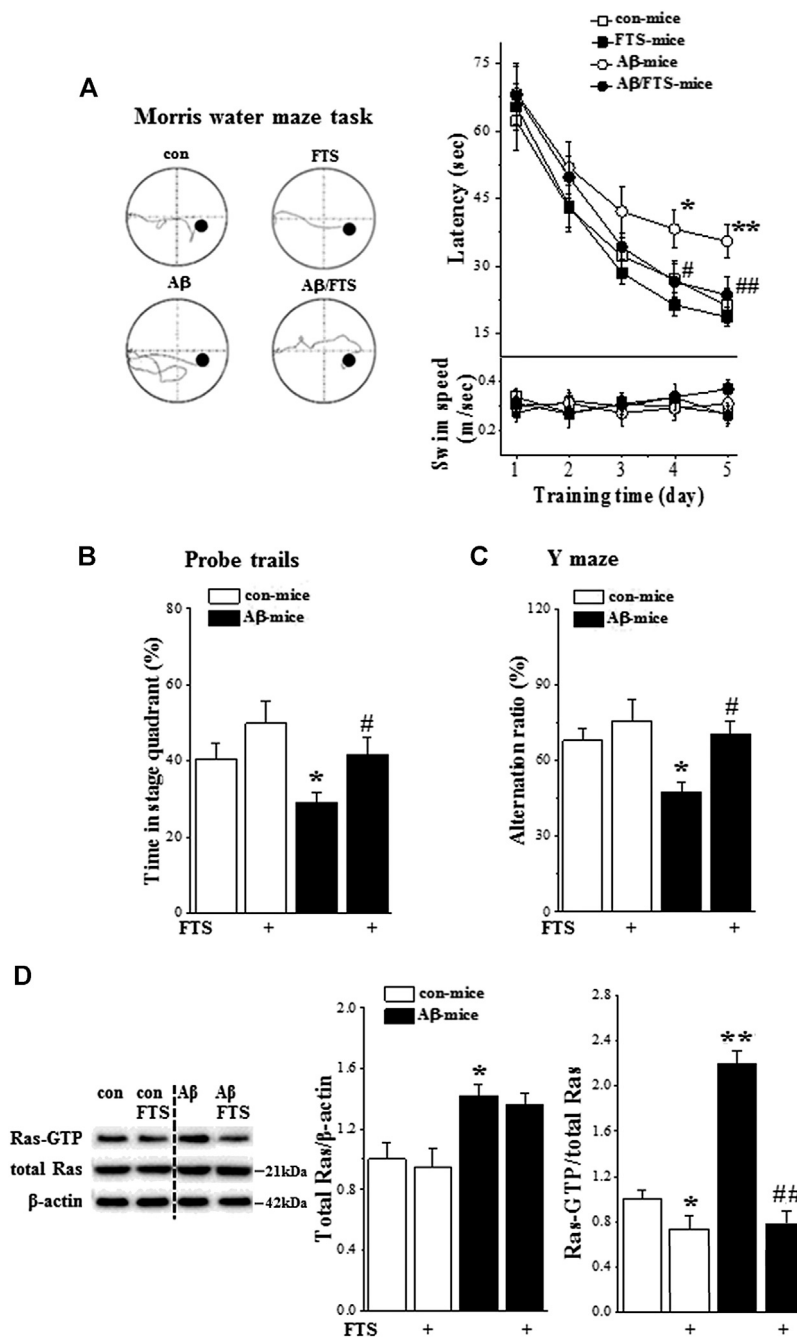
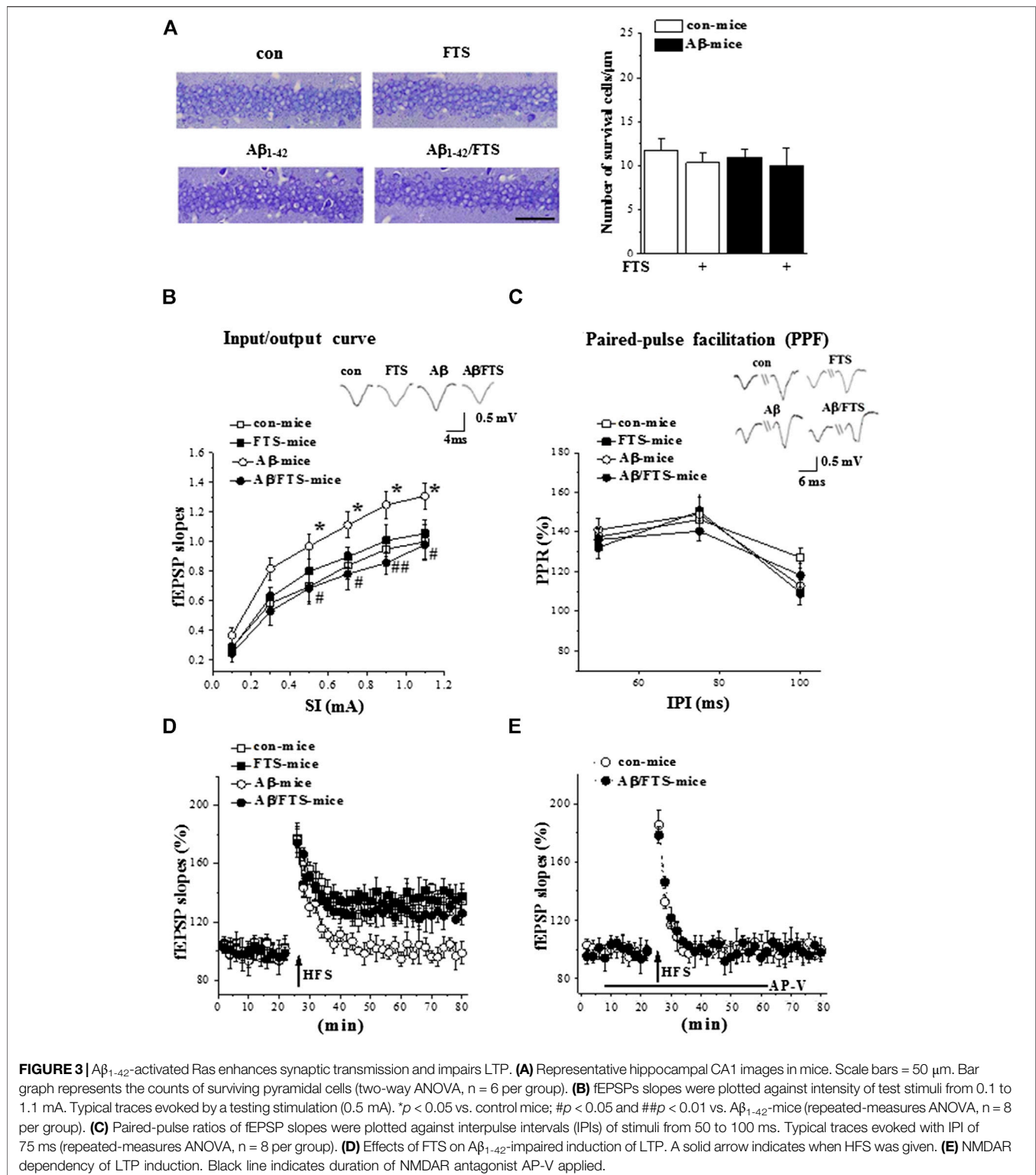


FIGURE 2 | $A\beta_{1-42}$ impairs spatial cognition via Ras hyperactivation. **(A)** Each point (upper panel) indicates group mean latency (sec) to reach the hidden-platform in control mice (con-mice), $A\beta_{1-42}$ -mice ($A\beta$ -mice), FTS-treated control mice (FTS-mice) and FTS-treated $A\beta_{1-42}$ -mice ($A\beta$ /FTS-mice). Each point (bottom panel) indicates mean swim speed (m/sec). Left panels show representative swimming tracks of mice searching for the underwater platform at day 5 after training. * $p < 0.05$ and ** $p < 0.01$ vs. control mice; # $p < 0.05$ and ## $p < 0.01$ vs. $A\beta_{1-42}$ -mice (repeated-measures ANOVA, $n = 8$ per group). **(B)** Bars present the percentage of time spent in target quadrant of probe trails. * $p < 0.05$ vs. control mice; # $p < 0.05$ vs. $A\beta_{1-42}$ -mice (two-way ANOVA, $n = 8$ per group). **(C)** Bar graph indicates group mean of alternation rate (%) in Y-maze task. * $p < 0.05$ vs. control mice; # $p < 0.05$ vs. $A\beta_{1-42}$ -mice (two-way ANOVA, $n = 8$ per group). **(D)** Effects of $A\beta_{1-42}$ on expression and activation of hippocampal Ras. Bar graphs represent the levels of total Ras protein and Ras-GTP in mice. The mean value per experimental group was normalized by control mice. * $p < 0.05$ and ** $p < 0.01$ vs. control mice; ## $p < 0.01$ vs. $A\beta_{1-42}$ -mice (two-way ANOVA, $n = 6$ per group).

influence of $A\beta_{1-42}$ on the expression and activity of hippocampal Ras ($n = 6$ per group). Compared with control mice, the level of Ras protein in $A\beta_{1-42}$ -mice was increased by approximately 30%

($p = 0.049$; **Figure 2D**) and the level of Ras-GTP was elevated at least 2-fold ($p < 0.001$). FTS has been demonstrated to selectively disrupt the interactions of active Ras proteins with the plasma



membrane (Elad-Sfadia et al., 2002). The administration of FTS (**Figure 1A**) not only reduced the level of Ras-GTP in control mice (FTS-mice, $p = 0.041$) but also prevented the increase in Ras-GTP in $A\beta_{1-42}$ -mice ($A\beta_{1-42}$ /FTS-mice, $p < 0.001$) with no change of Ras protein ($p > 0.05$).

Treatment of $A\beta$ -mice with FTS (**Figure 1A**) corrected the increase in escape latency in the MWM ($p = 0.009$) and the decline in swimming time in the target quadrant of the probe trial ($p = 0.032$). Subsequently, the alternation ratio in the Y-maze was restored in $A\beta_{1-42}$ /FTS-mice ($p = 0.027$). By contrast, FTS-mice

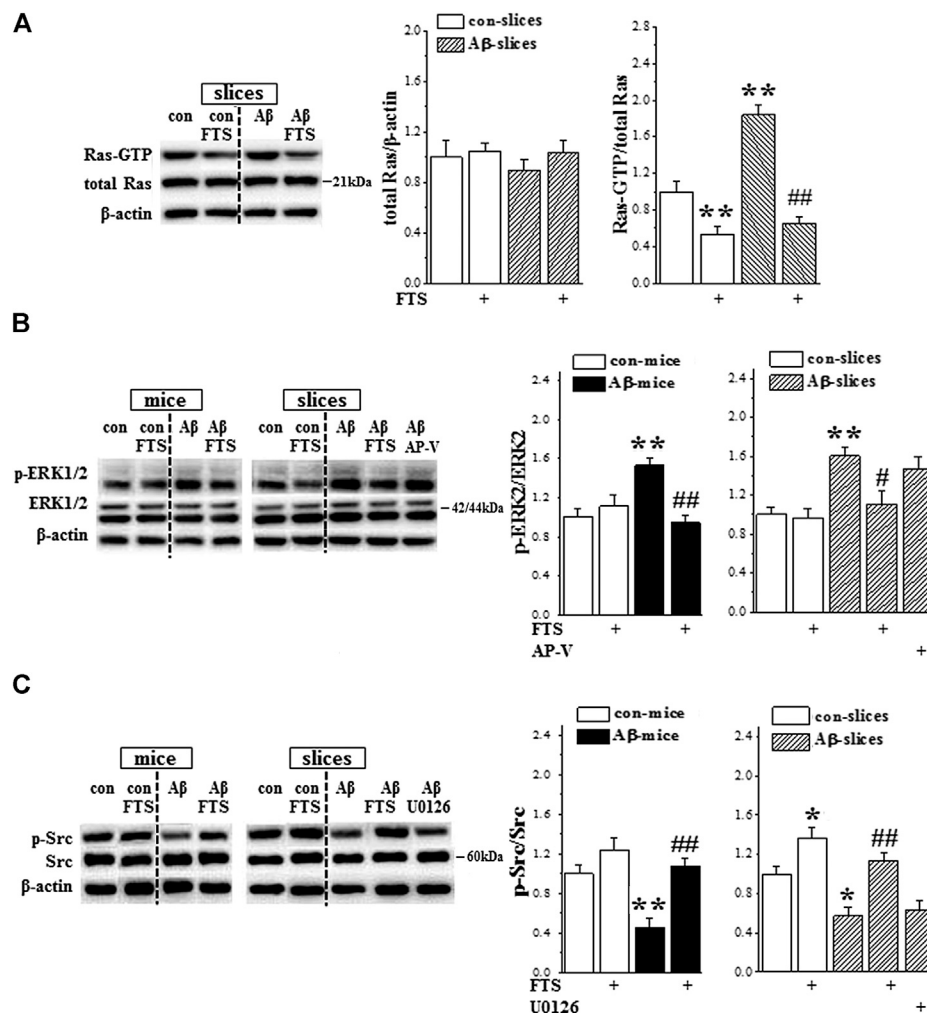


FIGURE 4 | A β_{1-42} -activated Ras enhances ERK signaling and suppresses Src activity. **(A)** Acute effect of A β_{1-42} on hippocampal Ras activity. Left panels show representative pictures of Western blot in control slices (con), FTS-slices (FTS), A β_{1-42} -slices (A β) and A β_{1-42} /FTS-slices (A β /FTS). Bar graphs represent the levels of Ras protein and Ras-GTP. The mean value per experimental group was normalized by control. ** $p < 0.01$ vs. control slices; ## $p < 0.01$ vs. A β_{1-42} -slices (two-way ANOVA, $n = 12$ per group). **(B)** and **(C)** Bar graphs show the levels of hippocampal ERK2 and Src phosphorylation (p-ERK2, p-Src) in control mice/slices (con), FTS-mice/slices (FTS), A β_{1-42} -mice/slices (A β) and A β_{1-42} /FTS-mice/slices (A β /FTS). * $p < 0.05$ and ** $p < 0.01$ vs. control mice/slices; # $p < 0.05$ and ## $p < 0.01$ vs. A β_{1-42} -mice/slices (two-way ANOVA, $n = 6$ mice or 12 slices per group).

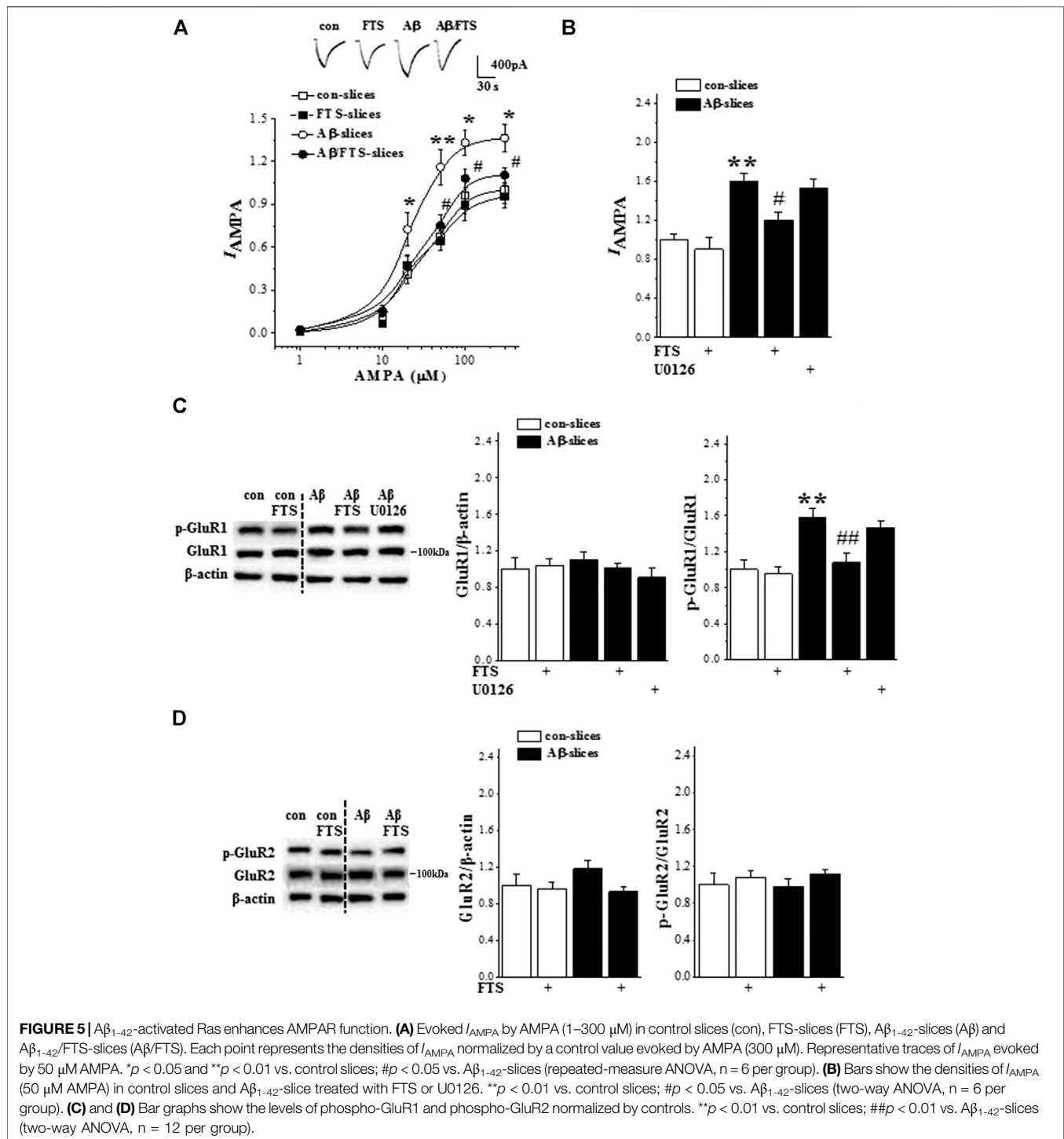
did not show changes in the escape latency of the MWM ($p > 0.05$), the swimming time of the target quadrant ($p > 0.05$) and the alternation ratio ($p > 0.05$).

3.2. A β_{1-42} -Activated Ras Enhances Synaptic Transmission and Impairs LTP

The counts of surviving pyramidal cells ($n = 6$ per group; **Figure 1A**) showed that the number of cells was unchanged in the hippocampal CA1 region of A β_{1-42} -mice ($p > 0.05$; **Figure 3A**), A β_{1-42} /FTS-mice ($p > 0.05$), and FTS-mice ($p > 0.05$) in comparison with control mice.

Subsequently, we examined the basal properties of hippocampal CA3-CA1 synaptic transmission and the induction of LTP by field potential recordings ($n = 8$ slices/4 mice per group). The input-output relationship was built by plotting the slope of field EPSP (fEPSP) vs. the intensities (0.1–1.1 mA) of stimulating

Schaffer collateral-commissural fibers. Compared with control mice, the A β_{1-42} -mice had increased fEPSP slopes ($F_{(1,14)} = 12.624$, $p = 0.003$; **Figure 3B**), which was corrected by FTS treatment ($F_{(1,14)} = 18.196$, $p = 0.001$). PPF was evoked by 0.5 mA two stimuli (50–100 ms IPI). The PPR of fEPSP slopes was not changed in A β_{1-42} mice ($p > 0.05$; **Figure 3C**) or A β_{1-42} /FTS mice ($p > 0.05$). The delivery of high-frequency stimuli (HFS, 100 Hz with 100 pulses) in control mice induced an about 40% increase in the fEPSP slopes (at 55–60 min after HFS; **Figure 3D**), which was blocked by AP-V. The application of the same HFS protocol in A β_{1-42} mice did not cause a long-lasting increase in the fEPSP slopes (**Figure 3E**). NMDAR-dependent LTP could be induced in A β_{1-42} /FTS mice. The fEPSP slopes ($p > 0.05$) and the PPR value ($p > 0.05$) in FTS-mice did not differ from those in control mice. The amplitude of NMDA-dependent LTP in FTS-mice failed to be increased compared with control mice (**Figure 3D**).



3.3. $A\beta_{1-42}$ -Activated Ras Enhances ERK Signaling and Suppresses Src Activity

Primary neurons treated with oligomeric $A\beta_{1-42}$ for 5 min exhibited a significant increase in Ras-ERK signaling activity (Kirouac et al., 2017). To explore the molecular mechanisms underlying $A\beta_{1-42}$ -impaired NMDAR-dependent LTP and $A\beta_{1-42}$ -enhanced postsynaptic response by the hyperactivity of Ras,

further experiments were conducted to detect the functions of AMPAR and NMDAR. First, the activity of Ras was examined in the hippocampal slices treated with $A\beta_{1-42}$ ($A\beta_{1-42}$ -slices), $A\beta_{1-42}$ /FTS ($A\beta_{1-42}$ /FTS-slices) or FTS (FTS-slices) for 60 min (n = 12 slices/4 mice per group; **Figure 1B**). In comparison with control, the level of Ras-GTP was significantly increased in $A\beta_{1-42}$ -slices (p < 0.001; **Figure 4A**),

which was sensitive to the addition of FTS ($p < 0.001$). The level of GTP-Ras was lower in FTS-slices ($p = 0.008$).

Subsequently, we examined the phosphorylation of ERK1/2 (phospho-ERK1/2) and Src (phospho-Src) in the hippocampus of $A\beta_{1-42}$ -mice (Figure 1A, $n = 6$ mice per group) or $A\beta_{1-42}$ -slices (Figure 1B, $n = 12$ slices/4 mice per group). The levels of phospho-ERK2 in $A\beta_{1-42}$ -mice ($p = 0.004$; Figure 4B) and $A\beta_{1-42}$ -slices ($p = 0.005$) were significantly increased without changes in the levels of ERK2 protein ($p > 0.05$). The increased phospho-ERK2 in $A\beta_{1-42}$ -mice ($p = 0.002$) and $A\beta_{1-42}$ -slices ($p = 0.026$) was corrected by the application of FTS, but not AP-V ($p > 0.05$). Notably, both $A\beta_{1-42}$ -mice ($p = 0.005$; Figure 4C) and $A\beta_{1-42}$ -slices ($p = 0.038$) showed a significant decline in the level of phospho-Src, which could be rescued by the application of FTS (mice: $p = 0.001$; slices: $p = 0.003$). In addition, the level of phospho-Src showed a slight increase in FTS-slices ($p = 0.037$), but not in FTS-mice ($p > 0.05$). The levels of phospho-ERK2 were not altered in both of FTS-mice and FTS-slices ($p > 0.05$).

3.4. $A\beta_{1-42}$ -Activated Ras Signaling Enhances AMPAR Function

Because the $A\beta_{1-42}$ -slices showed an increase in Ras activity, we further examined the response of AMPAR by whole cell patch-clamp recording ($n = 6$ cells/6 slices/4 mice per group). The application of AMPA in hippocampal slices evoked a dose-dependent inward current (I_{AMPA}) in CA1 pyramidal cells ($F_{(5,75)} = 136.706$, $p < 0.001$; Figure 5A). The densities of I_{AMPA} were increased in $A\beta_{1-42}$ -slices in comparison with control slices ($F_{(1,10)} = 32.619$, $p < 0.001$) but showed no difference between control slices and $A\beta_{1-42}$ /FTS-slices ($F_{(1,10)} = 2.680$, $p = 0.133$) or FTS-slices ($F_{(1,10)} = 0.198$, $p = 0.665$). Furthermore, the increased density of I_{AMPA} in $A\beta_{1-42}$ -slices ($p = 0.001$; Figure 5B) was corrected by the addition of FTS ($p = 0.043$) rather than the MAPK kinase (MEK) inhibitor U0126 ($p > 0.05$).

GluR1/2 protein and phosphorylation (phospho-GluR1, phospho-GluR2) were examined by Western blotting ($n = 12$ slices/4 mice per group). The level of GluR1 protein in $A\beta_{1-42}$ -slices did not differ significantly from that in control slices ($p > 0.05$; Figure 5C), but the level of phospho-GluR1 was increased ($p = 0.002$), which was blocked by the addition of FTS ($p = 0.009$) rather than U0126 ($p > 0.05$). The $A\beta_{1-42}$ -slices did not show changes in the level of GluR2 protein ($p > 0.05$; Figure 5D) or phospho-GluR2 ($p > 0.05$).

3.5. $A\beta_{1-42}$ -Activated Ras Inhibits NMDAR Function via Downregulation of Src

Subsequently, we examined NMDAR activity in hippocampal CA1 pyramidal cells ($n = 6$ cells/6 slices/4 mice per group). In the presence of AMPAR antagonist CNQX, the application of NMDA evoked an inward current (I_{NMDA}). The densities of I_{NMDA} showed a dose-dependent difference ($F_{(5,75)} = 73.185$, $p < 0.001$; Figure 6A). The densities of I_{NMDA} in $A\beta_{1-42}$ -slices were less than those in control slices ($F_{(1,10)} = 31.472$, $p < 0.001$), which was rescued by the addition of FTS ($p = 0.004$; Figure 6B) but not U0126 ($p > 0.05$). The protective effect of FTS on the

densities of I_{NMDA} in $A\beta_{1-42}$ -slices was sensitive to the use of PP2 ($p = 0.017$). In addition, the density of I_{NMDA} in FTS-slices was higher than in the control slices ($p = 0.026$), which was corrected by the use of PP2 ($p < 0.001$). Haas et al. (2002) reported previously that ouabain binding to the Na⁺/K⁺ + -ATPase activated Src kinase in several different cell lines. The exposure to 5 μ M ouabain for 30 min failed to increase the density of I_{NMDA} in control slices ($p > 0.05$). However, the treatment with ouabain could correct the density of I_{NMDA} in $A\beta_{1-42}$ -slices ($p = 0.043$), which was sensitive to PP2 ($p = 0.028$).

The phosphorylation of hippocampal GluN2B (phospho-GluN2B) and GluN2A (phospho-GluN2A) was further examined ($n = 12$ slices/4 mice per group). Compared with the controls, the levels of phospho-GluN2A ($p = 0.011$; Figure 6C) and phospho-GluN2B ($p = 0.040$; Figure 6D) were reduced in $A\beta_{1-42}$ -slices. The changes could be recovered by the use of FTS (phospho-GluN2A: $p = 0.003$; phospho-GluN2B: $p = 0.011$). The recovery of phospho-GluN2A ($p < 0.001$) or phospho-GluN2B ($p = 0.018$) in $A\beta_{1-42}$ /FTS-slices was blocked by the application of PP2. The level of phospho-GluN2A ($p = 0.021$) and phospho-GluN2B ($p = 0.046$) was increased in FTS-slices, which was sensitive to the addition of PP2 (phospho-GluN2A, $p < 0.001$; phospho-GluN2B, $p = 0.006$). Although the treatment with ouabain caused an increase in the phospho-GluN2A or phospho-GluN2B, the group when compared with control mice failed to reach the significance ($p > 0.05$). Notably, the application of ouabain could recover the levels of the phospho-GluN2A ($p = 0.041$) or phospho-GluN2B ($p = 0.048$) in $A\beta_{1-42}$ -slices, which were blocked by PP2 (GluN2A: $p = 0.034$; GluN2B: $p = 0.029$).

3.6. $A\beta_{1-42}$ -Activated Ras Impairs LTP and Spatial Cognition via Downregulation of Src

The chronic (three times a week) administration (i.p.) of a low dose (1 μ g/kg) of ouabain in mice improves functional recovery following traumatic brain injury (Dvela-Levitt et al., 2014). To confirm whether the hyperactivation of Ras through reducing Src activity impairs LTP induction and spatial cognition, $A\beta_{1-42}$ /FTS-mice and control mice were injected (i.c.v.) with PP2; $A\beta_{1-42}$ -mice were treated (i.p.) with 1 μ g/kg ouabain (Figure 1). The administration of PP2 ($n = 8$ slices/4 mice per group) did not alter fEPSP slopes in control mice ($p > 0.05$; Figure 7A) or $A\beta_{1-42}$ /FTS-mice ($p > 0.05$), but it suppressed the LTP induction in the both groups (Figure 7B). The fEPSP slopes were unchanged by the injection of ouabain (1 μ g/kg) in control mice ($p > 0.05$) or $A\beta_{1-42}$ -mice ($p > 0.05$). Importantly, the administration of ouabain could rescue the LTP induction in $A\beta_{1-42}$ -mice (Figure 7C), although it failed to alter the LTP induction in control mice.

The administration of PP2 in $A\beta_{1-42}$ /FTS-mice ($n = 8$ mice per group) prevented the protective effects of FTS on the escape latency of the MWM ($p = 0.038$; Figure 7D), the swimming time in the target quadrant of the probe trial ($p = 0.026$; Figure 7E) and the alternation ratio in the Y-maze ($p = 0.032$; Figure 7F). In addition, PP2-treated control mice showed deficits in spatial cognition, such as increased escape latency in the MWM ($p = 0.037$) and reduced swimming time in the target quadrant ($p = 0.031$) or alternation

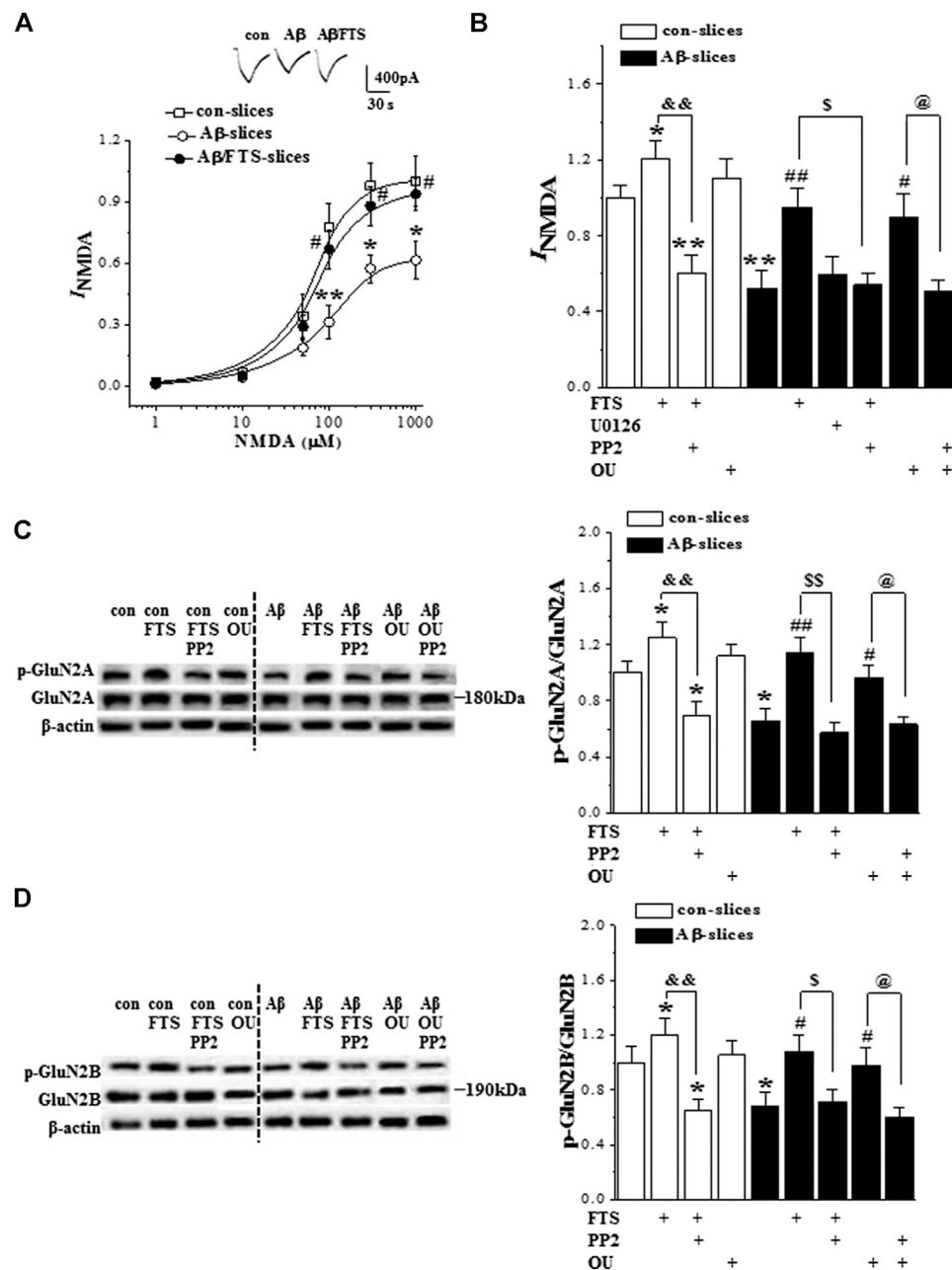
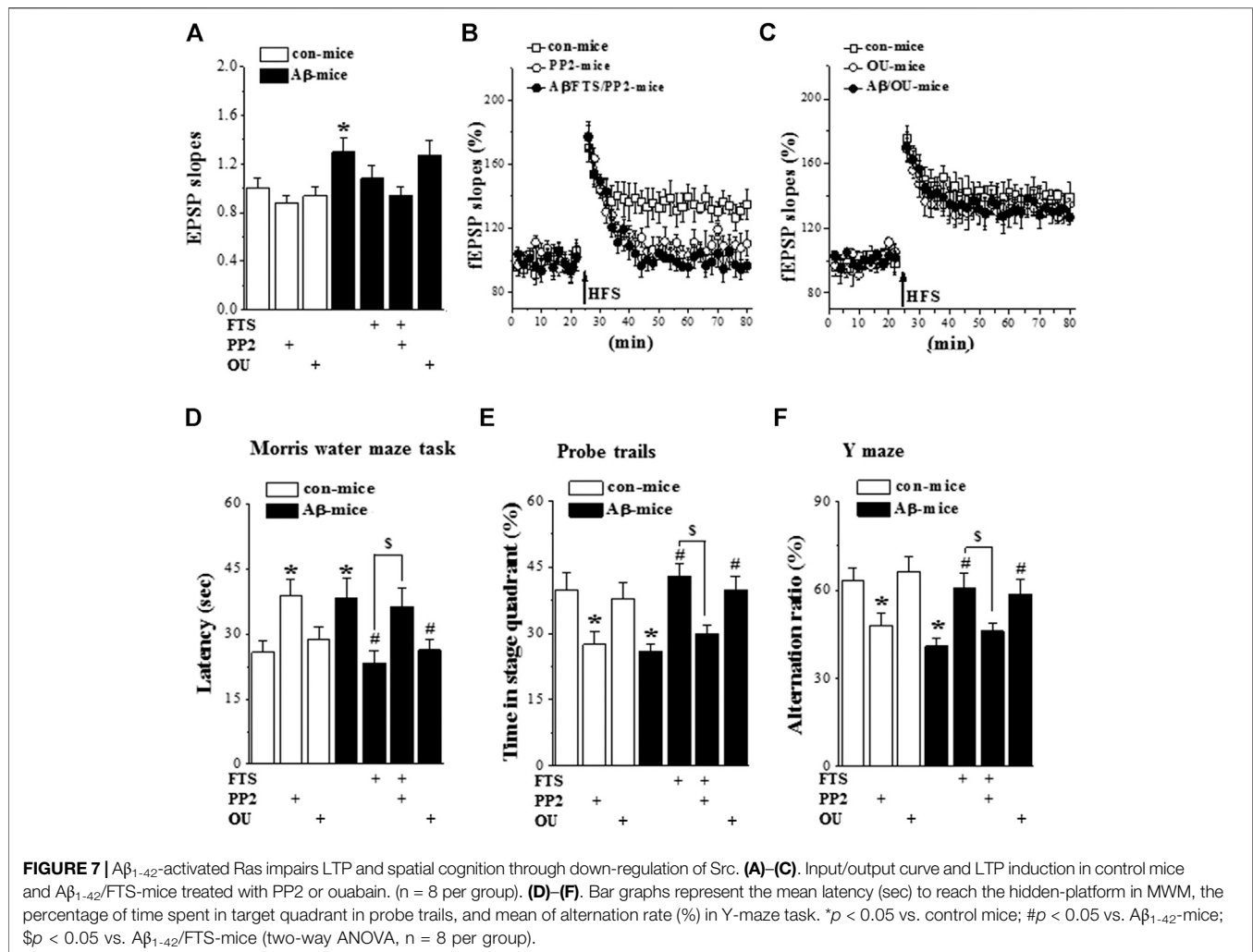


FIGURE 6 | $A\beta_{1-42}$ -activated Ras reduces NMDAR function via down-regulation of Src. **(A)** Evoked I_{NMDA} by NMDA (1–1,000 μM) in control slices (con), $A\beta_{1-42}$ -slices ($A\beta$) and $A\beta_{1-42}$ /FTS-slices ($A\beta$ /FTS). Each point represents the densities of I_{NMDA} normalized by control value evoked by NMDA (1,000 μM). Representative traces of I_{NMDA} evoked by 100 μM NMDA. * $p < 0.05$ and ** $p < 0.01$ vs. control slices; # $p < 0.05$ vs. $A\beta_{1-42}$ -slices (repeated-measure ANOVA, $n = 6$ per group). **(B)** Bars show the densities of I_{NMDA} (100 μM NMDA) in control slices and $A\beta_{1-42}$ -slices treated with FTS, U0126, PP2 or ouabain (OU). * $p < 0.05$ and ** $p < 0.01$ vs. control slices; # $p < 0.05$ and ## $p < 0.01$ vs. $A\beta_{1-42}$ -slices; && $p < 0.01$ vs. FTS-slices; \$ $p < 0.05$ vs. $A\beta_{1-42}$ /FTS-slices; @ $p < 0.05$ vs. $A\beta_{1-42}$ /OU-slices (two-way ANOVA, $n = 6$ per group). **(C)** and **(D)** Bar graphs show the levels of hippocampal phospho-GluN2A and phospho-GluN2B normalized by controls. * $p < 0.05$ vs. control slices; # $p < 0.05$ and ## $p < 0.01$ vs. $A\beta_{1-42}$ -slices; and& $p < 0.01$ vs. FTS-slices; \$ $p < 0.05$ and \$\$ $p < 0.01$ vs. $A\beta_{1-42}$ /FTS-slices; @ $p < 0.05$ vs. $A\beta_{1-42}$ /OU-slices (two-way ANOVA, $n = 12$ per group).

ratio ($p = 0.045$). The treatment with ouabain in $A\beta_{1-42}$ -mice recovered the escape latency of the MWM ($p = 0.034$), the swimming time in the target quadrant of the probe trial ($p = 0.041$) and the alternation ratio in the Y-maze ($p = 0.048$), whereas it did not affect the spatial cognition in control mice ($p > 0.05$).

4. DISCUSSION

The injection (i.c.v.) of mice with $A\beta_{1-42}$ or acute bath application of $A\beta_{1-42}$ in hippocampal slices could elevate hippocampal Ras activation. The oligomeric $A\beta_{1-42}$ impaired spatial cognition and



hippocampal LTP induction, which were improved by the administration of FTS. These results manifest that the oligomeric A β_{1-42} impairs spatial cognition *via* the hyperactivation of Ras.

In the hippocampus of A β_{1-42} -mice, the level of Ras protein was increased by approximately 30%, while the level of Ras-GTP was elevated at least 2-fold. In hippocampal slices, the 60 min bath application of A β_{1-42} could enhance the activation of Ras, although it failed to alter the level of Ras protein. The results provide a clear indication that oligomeric A β_{1-42} not only enhances Ras expression but also stimulates Ras activation. Because A β binds to specific neuronal membrane APP, it has been suggested that APP is a possible receptor for A β (Lorenzo et al., 2000). A β can induce phosphorylation on APP to enhance APP proteolysis (Kirouac et al., 2017). The cytoplasmic YENPTY motif of APP is known to be a docking site for the adaptor proteins Shc and Grb2, which recruit the GEF SOS2 for activation and expression of Ras (Kirouac et al., 2017). Andras and Toborek (2013) reported that treatment with A β (1 μ M) for 3 min caused redistribution of lipid rafts and caveola, which elevated the level of Ras-GTP. Acute treatment with A β_{1-42} can cascade ERK signaling in hippocampal neurons (Dineley et al., 2001). APP can positively regulate the Ras-ERK

signal pathways in neuronal cell lines (Chaput et al., 2012). York et al. (1998) reported that ERK can be persistently activated by the formation of a stable upstream complex between small G proteins. In this study, either *in vivo* or *in vitro* (60 min) treatment with A β_{1-42} caused an increase in the levels of hippocampal ERK2 phosphorylation without changes in the expression levels, which were sensitive to Ras inhibition. The Ras isoform H-Ras may contribute to the long-lasting activation of ERK2 (Krapivinsky et al., 2003). It is conceivable that A β_{1-42} , through the hyperactivation of Ras, causes a rapid and sustained increase in the ERK signaling. The activation of NMDAR-mediated CaMKII can cascade the Ras-ERK signaling pathway (Carlisle et al., 2008). However, NMDAR function was downregulated in A β_{1-42} -slices, and the blockade of NMDAR did not affect ERK2 phosphorylation. Dineley et al. (Dineley et al., 2001) reported, in the hippocampus, that chronic exposure to A β_{1-42} increased $\alpha 7$ nicotinic acetylcholine receptor (nAChR) protein, which led to chronic stimulation of ERK2. Therefore, whether A β_{1-42} -induced hyperactivation of Ras increases ERK2 phosphorylation through enhanced $\alpha 7$ nAChR function should be an interesting topic for future work.

The basal transmission of hippocampal CA3-CA1 synapses was enhanced in $A\beta_{1-42}$ -mice with no change in the capability of presynaptic glutamate release which depended on the hyperactivation of Ras rather than ERK. Postsynaptic AMPAR plays an important role in hippocampal synaptic transmission (Schwenk et al., 2014). AMPAR is synthesized dendritically and inserted into the synaptic membrane (Ju et al., 2004). The 60 min application of $A\beta_{1-42}$ caused an obvious increase in AMPAR function and GluR1 phosphorylation, which were sensitive to Ras inhibition. The hyperactivation of Ras drives the synaptic insertion of AMPAR by triggering the phosphorylation of GluR1 at S845 and S831 (Zhu et al., 2002). Manabe et al. (2000) reported that the AMPAR synaptic responses were unchanged in CA1 pyramidal neurons of H-Ras knockout mice. Qin et al. (2005) found that the ERK1/2 phosphorylation and subsequent activation of CREB can increase AMPAR function. Enhanced ERK activity increases the expression of the GluR1 subunits (Schumann and Yaka 2009). The decline in CREB phosphorylation caused a specific downregulation of postsynaptic GluR1 (Borges and Dingleline 2001). However, the increases in AMPAR function and GluR1 phosphorylation in $A\beta_{1-42}$ -slices were insensitive to the inhibition of MEK. Furthermore, the levels of GluR1 proteins in $A\beta_{1-42}$ -slices were unchanged. A-type K^+ channels have been reported to be a substrate of ERK1/2 (Schrader et al., 2006). The phosphorylation of K^+ channels is known to be a primary mechanism for the ERK1/2-decreased A-type currents (Yuan et al., 2006). We observed that the inhibition of MEK failed to alter the increased fEPSP slopes in $A\beta_{1-42}$ -mice (data not shown).

NMDARs are linked to cognitive impairments in AD (Goussakov et al., 2010). The expression of GluN2A and GluN2B was downregulated in AD patient brains (Hynd et al., 2004). $A\beta$ can induce the dysfunction of hippocampal NMDAR via the inactivation of GluN2B (Yin et al., 2015). The NMDAR activation is negatively regulated by the Ras signaling (Li et al., 2005). H-Ras overexpression decreases tyrosine phosphorylation of NMDAR GluN2A (Thornton et al., 2003). By inhibiting RACK1, a Ras effector protein, NMDAR currents in hippocampal neurons were increased (Yaka et al., 2002). Ras activation induces a decline in the Src autophosphorylation (Thornton et al., 2003). Src tyrosine phosphorylation positively regulates NMDAR channel activity (Sha et al., 2015). We observed that the 60 min application of $A\beta_{1-42}$ suppressed the phosphorylation of Src and GluN2A/2B, leading to NMDAR dysfunction, which could be corrected by the inhibition of Ras or the activation of Src rather than the inactivation of MEK. The deficits in hippocampal NMDAR-dependent LTP and spatial cognition in $A\beta_{1-42}$ -mice could be rescued by the inhibition of Ras. The inhibition of Src not only reduced the phosphorylation of GluN2A/2B and NMDAR activity and depressed LTP induction and spatial cognition in control mice, but also blocked the NMDAR-dependent LTP and spatial cognition in $A\beta_{1-42}$ -mice treated with the Ras inhibitor. Moreover, the administration of Src activator at a low dose could rescue the $A\beta$ -impaired spatial cognition and NMDAR-dependent LTP. In addition, treatment of rat brain slices with Tat-H-Ras decreased Src phosphorylation of GluN2A, and decreased the magnitude of

hippocampal LTP (Thornton et al., 2003). The induction of hippocampal NMDAR-dependent LTP has been widely thought to be the basis for explicit memory formation and storage (McGaugh 2000). Thus, the results in this study give an indication that $A\beta_{1-42}$ through suppressed Src activation blocks NMDAR-dependent LTP induction leading to impairment of spatial cognition. Ras-ERK signaling is considered to be critical for LTP induction (Patterson et al., 2010) since the inhibition of Ras or ERK blocks LTP induction (Zhu et al., 2002). Ras-ERK signaling is reported to induce the activation of L voltage-sensitive Ca^{2+} channel (L-VGCC) (Ekinici et al., 1999), which can enhance L-VGCC-dependent LTP (Moosmang et al., 2005).

5. CONCLUSION

The isoprenylated GTPases have been associated with the pathogenesis of AD (Ostrowski et al., 2007; Scheper et al., 2007). Ras levels are increased in brains with AD (McShea et al., 2007). In the current study, we provided the first *in vivo* and *in vitro* evidence that the $A\beta_{1-42}$ -induced abnormal increase in Ras activity may account for the impairment of NMDAR-dependent LTP induction and spatial cognition through the downregulation of Src, suggesting that targeting Ras signaling may be an effective strategy to protect hippocampal synaptic plasticity against $A\beta$ -induced cognitive decline at early stages of AD.

DATA AVAILABILITY STATEMENT

The original contributions presented in the study are included in the article/**Supplementary Material**, further inquiries can be directed to the corresponding author.

ETHICS STATEMENT

The animal study was reviewed and approved by Ethical Committee of the Nanjing Medical University.

AUTHOR CONTRIBUTIONS

YW performed the electrophysiological experiments and the preparation of the manuscript. ZS performed all statistical analysis. YZ undertook the western blot analysis. JY carried out the animal care and the behavioral examinations. LC and WY carried out the experimental design and revision of the manuscript.

ACKNOWLEDGMENTS

This study was supported by the National Natural Science Foundation of China (81471157); Special Grant for Central Government Supporting Local Science and Technology

Development, Science and Technology Department of Guizhou Province (2019-4008); Special Funds of Jiangsu Provincial Key Research and Development Projects (BE2019612); Jiangsu Provincial Cadre Health Research Projects (BJ17006).

REFERENCES

Andras, I. E. and Toborek, M. (2013). Amyloid beta accumulation in HIV-1-infected brain: the role of the blood brain barrier. *IUBMB Life* 65 (1), 43–49. doi:10.1002/iub.1106

Borges, K. and Dingledine, R. (2001). Functional organization of the GluR1 glutamate receptor promoter. *J. Biol. Chem.* 276 (28), 25929–25938. doi:10.1074/jbc.M009105200

Bouter, Y., Dietrich, K., Wittnam, J. L., Rezaei-Ghaleh, N., Pillot, T., Papot-Couturier, S., et al. (2013). N-truncated amyloid beta (Abeta) 4–42 forms stable aggregates and induces acute and long-lasting behavioral deficits. *Acta Neuropathol.* 126 (2), 189–205. doi:10.1007/s00401-013-1129-2

Carlisle, H. J., Manzerra, P., Marcora, E., and Kennedy, M. B. (2008). SynGAP regulates steady-state and activity-dependent phosphorylation of cofilin. *J. Neurosci.* 28 (50), 13673–13683. doi:10.1523/JNEUROSCI.4695-08.2008

Chaput, D., Kirouac, L. H., Bell-Temin, H., Stevens, S. M., Jr., and Padmanabhan, J. (2012). SILAC-based proteomic analysis to investigate the impact of amyloid precursor protein expression in neuronal-like B103 cells. *Electrophoresis* 33 (24), 3728–3737. doi:10.1002/elps.201200251

Chen, T., Zhang, B., Li, G., Chen, L., and Chen, L. (2016). Simvastatin enhances NMDA receptor GluN2B expression and phosphorylation of GluN2B and GluN2A through increased histone acetylation and Src signaling in hippocampal CA1 neurons. *Neuropharmacology* 107, 411–421. doi:10.1016/j.neuropharm.2016.03.028

Cui, Y., Costa, R. M., Murphy, G. G., Elgersma, Y., Zhu, Y., Gutmann, D. H., et al. (2008). Neurofibromin regulation of ERK signaling modulates GABA release and learning. *Cell* 135 (3), 549–560. doi:10.1016/j.cell.2008.09.060

Dawson, M. R., Polito, A., Levine, J. M., and Reynolds, R. (2003). NG2-expressing glial progenitor cells: an abundant and widespread population of cycling cells in the adult rat CNS. *Mol. Cell. Neurosci.* 24 (2), 476–488. doi:10.1016/s1044-7431(03)00210-0

Dineley, K. T., Westerman, M., Bui, D., Bell, K., Ashe, K. H., and Sweatt, J. D. (2001). Beta-amyloid activates the mitogen-activated protein kinase cascade via hippocampal alpha7 nicotinic acetylcholine receptors: in vitro and in vivo mechanisms related to Alzheimer's disease. *J. Neurosci.* 21 (12), 4125–4133.

Dvella-Levitt, M., Ami, H. C., Rosen, H., Shohami, E., and Lichtstein, D. (2014). Ouabain improves functional recovery following traumatic brain injury. *J. Neurotrauma* 31 (23), 1942–1947. doi:10.1089/neu.2014.3544

Ekinci, F. J., Malik, K. U., and Shea, T. B. (1999). Activation of the L voltage-sensitive calcium channel by mitogen-activated protein (MAP) kinase following exposure of neuronal cells to beta-amyloid. MAP kinase mediates beta-amyloid-induced neurodegeneration. *J. Biol. Chem.* 274 (42), 30322–30327. doi:10.1074/jbc.274.42.30322

Elad-Sfadia, G., Haklai, R., Ballan, E., Gabius, H. J., and Kloog, Y. (2002). Galectin-1 augments Ras activation and diverts Ras signals to Raf-1 at the expense of phosphoinositide 3-kinase. *J. Biol. Chem.* 277 (40), 37169–37175. doi:10.1074/jbc.M205698200

Ferrer, I., Blanco, R., Carmona, M., and Puig, B. (2001). Phosphorylated c-MYC expression in Alzheimer disease, Pick's disease, progressive supranuclear palsy and corticobasal degeneration. *Neuropathol. Appl. Neurobiol.* 27 (5), 343–351. doi:10.1046/j.1365-2990.2001.00348.x

Gartner, U., Holzer, M., and Arendt, T. (1999). Elevated expression of p21ras is an early event in Alzheimer's disease and precedes neurofibrillary degeneration. *Neuroscience* 91 (1), 1–5. doi:10.1016/s0306-4522(99)00059-7

Goussakov, I., Miller, M. B., and Stutzmann, G. E. (2010). NMDA-mediated Ca(2+) influx drives aberrant ryanodine receptor activation in dendrites of young Alzheimer's disease mice. *J. Neurosci.* 30 (36), 12128–12137. doi:10.1523/JNEUROSCI.2474-10.2010

SUPPLEMENTARY MATERIAL

The Supplementary Material for this article can be found online at: <https://www.frontiersin.org/articles/10.3389/fphar.2020.595360/full#supplementary-material>.

Haas, M., Wang, H., Tian, J., and Xie, Z. (2002). Src-mediated inter-receptor cross-talk between the Na⁺/K⁺-ATPase and the epidermal growth factor receptor relays the signal from ouabain to mitogen-activated protein kinases. *J. Biol. Chem.* 277 (21), 18694–18702. doi:10.1074/jbc.M111357200

Hynd, M. R., Scott, H. L., and Dodd, P. R. (2004). Differential expression of N-methyl-D-aspartate receptor NR2 isoforms in Alzheimer's disease. *J. Neurochem.* 90 (4), 913–919. doi:10.1111/j.1471-4159.2004.02548.x

Jin, H., Chen, T., Li, G., Wang, C., Zhang, B., Cao, X., et al. (2016). Dose-dependent neuroprotection and neurotoxicity of simvastatin through reduction of farnesyl pyrophosphate in mice treated with intracerebroventricular injection of Abeta 1–42. *J. Alzheim. Dis.* 50 (2), 501–516. doi:10.3233/JAD-150782

Ju, W., Morishita, W., Tsui, J., Gaietta, G., Deerinck, T. J., Adams, S. R., et al. (2004). Activity-dependent regulation of dendritic synthesis and trafficking of AMPA receptors. *Nat. Neurosci.* 7 (3), 244–253. doi:10.1038/nn1189

Karni, R., Mizrachi, S., Reiss-Sklan, E., Gazit, A., Livnah, O., and Levitzki, A. (2003). The pp60c-Src inhibitor PP1 is non-competitive against ATP. *FEBS Letters* 537 (1–3), 47–52. doi:10.1016/s0014-5793(03)00069-3

Kirouac, L., Rajic, A. J., Cribbs, D. H., and Padmanabhan, J. (2017). Activation of ras-ERK signaling and GSK-3 by amyloid precursor protein and amyloid beta facilitates neurodegeneration in Alzheimer's disease. *eNeuro* 4 (2). doi:10.1523/ENEURO.0149-16.2017

Kloog, Y., Cox, A. D., and Sinensky, M. (1999). Concepts in ras-directed therapy. *Expert Opin. Invest. Drugs* 8 (12), 2121–2140. doi:10.1517/13543784.8.12.2121

Krapivinsky, G., Krapivinsky, L., Manasian, Y., Ivanov, A., Tyzio, R., Pellegrino, C., et al. (2003). The NMDA receptor is coupled to the ERK pathway by a direct interaction between NR2B and RasGRF1. *Neuron* 40 (4), 775–784. doi:10.1016/s0896-6273(03)00645-7

Li, W., Cui, Y., Kushner, S. A., Brown, R. A. M., Jentsch, J. D., Frankland, P. W., et al. (2005). The HMG-CoA reductase inhibitor lovastatin reverses the learning and attention deficits in a mouse model of neurofibromatosis type 1. *Curr. Biol.* 15 (21), 1961–1967. doi:10.1016/j.cub.2005.09.043

Lorenzo, A., Yuan, M., Zhang, Z., Paganetti, P. A., Sturchler-Pierrat, C., Staufenbiel, M., et al. (2000). Amyloid β interacts with the amyloid precursor protein: a potential toxic mechanism in Alzheimer's disease. *Nat. Neurosci.* 3 (5), 460–464. doi:10.1038/74833

Manabe, T., Aiba, A., Yamada, A., Ichise, T., Sakagami, H., Kondo, H., et al. (2000). Regulation of long-term potentiation by H-Ras through NMDA receptor phosphorylation. *J. Neurosci.* 20 (7), 2504–2511. doi:10.1523/JNEUROSCI.20-07-02504.2000

McGaugh, J. L. (2000). Memory—a century of consolidation. *Science* 287 (5451), 248–251. doi:10.1126/science.287.5451.248

McShea, A., Lee, H. G., Petersen, R. B., Casadesu, G., Vincent, I., Linford, N. J., et al. (2007). Neuronal cell cycle re-entry mediates Alzheimer disease-type changes. *Biochim. Biophys. Acta* 1772 (4), 467–472. doi:10.1016/j.bbdis.2006.09.010

Moosmang, S., Haider, N., Klugbauer, N., Adelsberger, H., Langwieser, N., Müller, J., et al. (2005). Role of hippocampal Cav1.2 Ca²⁺ channels in NMDA receptor-independent synaptic plasticity and spatial memory. *J. Neurosci.* 25 (43), 9883–9892. doi:10.1523/JNEUROSCI.1531-05.2005

Niv, H., Gutman, O., Kloog, Y., and Henis, Y. I. (2002). Activated K-Ras and H-Ras display different interactions with saturable nonraft sites at the surface of live cells. *J. Cell Biol.* 157 (5), 865–872. doi:10.1083/jcb.200202009

North, K., Hyman, S., and Barton, B. (2002). Cognitive deficits in neurofibromatosis 1. *J. Child Neurol.* 17 (8), 605–612. doi:10.1177/088307380201700811

Ohno, M., Frankland, P. W., Chen, A. P., Costa, R. M., and Silva, A. J. (2001). Inducible, pharmacogenetic approaches to the study of learning and memory. *Nat. Neurosci.* 4 (12), 1238–1243. doi:10.1038/nn771

Ostrowski, S. M., Wilkinson, B. L., Golde, T. E., and Landreth, G. (2007). Statins reduce amyloid-beta production through inhibition of protein

- isoprenylation. *J. Biol. Chem.* 282 (37), 26832–26844. doi:10.1074/jbc.M702640200
- Patterson, M. A., Szatmari, E. M., and Yasuda, R. (2010). AMPA receptors are exocytosed in stimulated spines and adjacent dendrites in a Ras-ERK-dependent manner during long-term potentiation. *Proc. Natl. Acad. Sci. U.S.A.* 107 (36), 15951–15956. doi:10.1073/pnas.0913875107
- Pei, J. J., Braak, H., An, W. L., Winblad, B., Cowburn, R. F., Iqbal, K., et al. (2002). Up-regulation of mitogen-activated protein kinases ERK1/2 and MEK1/2 is associated with the progression of neurofibrillary degeneration in Alzheimer's disease. *Mol. Brain Res.* 109 (1–2), 45–55. doi:10.1016/s0169-328x(02)00488-6
- Prior, I. A. and Hancock, J. F. (2012). Ras trafficking, localization and compartmentalized signalling. *Semin. Cell Dev. Biol.* 23 (2), 145–153. doi:10.1016/j.semcdb.2011.09.002
- Qian, Y., Yin, J., Hong, J., Li, G., Zhang, B., Liu, G., et al. (2016). Neuronal seipin knockout facilitates Abeta-induced neuroinflammation and neurotoxicity via reduction of PPARgamma in hippocampus of mouse. *J. Neuroinflamm.* 13 (1), 145. doi:10.1186/s12974-016-0598-3
- Qin, Y., Zhu, Y., Baumgart, J. P., Stornetta, R. L., Seidenman, K., Mack, V., et al. (2005). State-dependent Ras signaling and AMPA receptor trafficking. *Genes Dev.* 19 (17), 2000–2015. doi:10.1101/gad.342205
- Scheper, W., Hoozemans, J. J., Hoogenraad, C. C., Rozemuller, A. J., Eikelenboom, P., and Baas, F. (2007). Rab6 is increased in Alzheimer's disease brain and correlates with endoplasmic reticulum stress. *Neuropathol. Appl. Neurobiol.* 33 (5), 523–532. doi:10.1111/j.1365-2990.2007.00846.x
- Schrader, L. A., Birnbaum, S. G., Nadin, B. M., Ren, Y., Bui, D., Anderson, A. E., et al. (2006). ERK/MAPK regulates the Kv4.2 potassium channel by direct phosphorylation of the pore-forming subunit. *Am. J. Physiol. Cell Physiol.* 290 (3), C852–C861. doi:10.1152/ajpcell.00358.2005
- Schumann, J., Alexandrovich, G. A., Biegon, A., and Yaka, R. (2008). Inhibition of NR2B phosphorylation restores alterations in NMDA receptor expression and improves functional recovery following traumatic brain injury in mice. *J. Neurotrauma* 25 (8), 945–957. doi:10.1089/neu.2008.0521
- Schumann, J. and Yaka, R. (2009). Prolonged withdrawal from repeated noncontingent cocaine exposure increases NMDA receptor expression and ERK activity in the nucleus accumbens. *J. Neurosci.* 29 (21), 6955–6963. doi:10.1523/JNEUROSCI.1329-09.2009
- Schwenk, J., Baehrens, D., Haupt, A., Bildl, W., Boudkazi, S., Roeper, J., et al. (2014). Regional diversity and developmental dynamics of the AMPA-receptor proteome in the mammalian brain. *Neuron* 84 (1), 41–54. doi:10.1016/j.neuron.2014.08.044
- Sha, S., Hong, J., Qu, W. J., Lu, Z. H., Li, L., Yu, W. F., et al. (2015). Sex-related neurogenesis decrease in hippocampal dentate gyrus with depressive-like behaviors in sigma-1 receptor knockout mice. *Eur. Neuropsychopharmacol.* 25 (8), 1275–1286. doi:10.1016/j.euroneuro.2015.04.021
- Shohami, E., Yatsiv, I., Alexandrovich, A., Haklai, R., Elad-Sfadia, G., Grossman, R., et al. (2003). The Ras inhibitor S-trans, trans-farnesylthiosalicylic acid exerts long-lasting neuroprotection in a mouse closed head injury model. *J. Cerebr. Blood Flow Metabol.* 23 (6), 728–738. doi:10.1097/01.WCB.0000067704.86573.83
- Stornetta, R. L. and Zhu, J. J. (2011). Ras and Rap signaling in synaptic plasticity and mental disorders. *Neuroscientist* 17 (1), 54–78. doi:10.1177/1073858410365562
- Thornton, C., Yaka, R., Dinh, S., and Ron, D. (2003). H-Ras modulates N-methyl-D-aspartate receptor function via inhibition of Src tyrosine kinase activity. *J. Biol. Chem.* 278 (26), 23823–23829. doi:10.1074/jbc.M302389200
- Tian, J., Cai, T., Yuan, Z., Wang, H., Liu, L., Haas, M., et al. (2006). Binding of Src to Na⁺/K⁺-ATPase forms a functional signaling complex. *Mol. Biol. Cell* 17 (1), 317–326. doi:10.1091/mbc.e05-08-0735
- Wang, Y., Chen, T., Yuan, Z., Zhang, Y., Zhang, B., Zhao, L., et al. (2018). Ras inhibitor S-trans, trans-farnesylthiosalicylic acid enhances spatial memory and hippocampal long-term potentiation via up-regulation of NMDA receptor. *Neuropharmacology* 139, 257–267. doi:10.1016/j.neuropharm.2018.03.026
- Yaka, R., Thornton, C., Vagts, A. J., Phamluong, K., Bonci, A., and Ron, D. (2002). NMDA receptor function is regulated by the inhibitory scaffolding protein, RACK1. *Proc. Natl. Acad. Sci. U.S.A.* 99 (8), 5710–5715. doi:10.1073/pnas.062046299
- Ye, X. and Carew, T. J. (2010). Small G protein signaling in neuronal plasticity and memory formation: the specific role of Ras family proteins. *Neuron* 68 (3), 340–361. doi:10.1016/j.neuron.2010.09.013
- Yin, J., Sha, S., Chen, T., Wang, C., Hong, J., Jie, P., et al. (2015). Sigma-1 (σ_1) receptor deficiency reduces beta-amyloid(25–35)-induced hippocampal neuronal cell death and cognitive deficits through suppressing phosphorylation of the NMDA receptor NR2B. *Neuropharmacology* 89, 215–224. doi:10.1016/j.neuropharm.2014.09.027
- York, R. D., Yao, H., Dillon, T., Eilig, C. L., Eckert, S. P., McCleskey, E. W., et al. (1998). Rap1 mediates sustained MAP kinase activation induced by nerve growth factor. *Nature* 392 (6676), 622–626. doi:10.1038/33451
- Yuan, L. L., Chen, X., Kunjilwar, K., Pfaffinger, P., and Johnston, D. (2006). Acceleration of K⁺ channel inactivation by MEK inhibitor U0126. *Am. J. Physiol. Cell Physiol.* 290 (1), C165–C171. doi:10.1152/ajpcell.00206.2005
- Zhou, L., Chen, T., Li, G., Wu, C., Wang, C., Li, L., et al. (2016). Activation of PPARgamma Ameliorates spatial cognitive deficits through restoring expression of AMPA receptors in seipin knock-out mice. *J. Neurosci.* 36 (4), 1242–1253. doi:10.1523/JNEUROSCI.3280-15.2016
- Zhu, J. J., Qin, Y., Zhao, M., Van Aelst, L., and Malinow, R. (2002). Ras and Rap control AMPA receptor trafficking during synaptic plasticity. *Cell* 110 (4), 443–455. doi:10.1016/s0092-8674(02)00897-8

Conflict of Interest: The authors declare that the research was conducted in the absence of any commercial or financial relationships that could be construed as a potential conflict of interest.

Copyright © 2020 Wang, Shi, Zhang, Yan, Yu and Chen. This is an open-access article distributed under the terms of the Creative Commons Attribution License (CC BY). The use, distribution or reproduction in other forums is permitted, provided the original author(s) and the copyright owner(s) are credited and that the original publication in this journal is cited, in accordance with accepted academic practice. No use, distribution or reproduction is permitted which does not comply with these terms.

GLOSSARY

AD Alzheimer's disease

A β amyloid beta

AMPA AMPA receptor

DMSO dimethyl sulfoxide

EPSP excitatory postsynaptic potential

FTS farnesylthiosalicylic acid

HFS high-frequency stimulation

LTP long-term potentiation

MWM Morris water maze

NMDAR NMDA receptor